Jarelh GALDOS [0000-0001-6591-1866]*, *Nikolai LOPEZ* [0000-0002-5748-0717]*,
Angie MEDINA [0000-0003-1046-7299]*, *Jorge HUARCA* [0000-0001-6300-5122]*,
Jorge RENDULICH [0000-0003-1302-547X]*, *Erasmo SULLA* [0000-0002-1223-1223]*

COMPARISON AND EVALUATION OF LMS-DERIVED ALGORITHMS APPLIED ON ECG SIGNALS CONTAMINATED WITH MOTION ARTIFACT DURING PHYSICAL ACTIVITIES

Abstract

The acquisition of ECG signals offers physicians and specialists a very important tool in the diagnosis of cardiovascular diseases. However, very often these signals are affected by noise from various sources, including noise generated by movement during physical activity. This type of noise is known as Motion Artifact (MA) which changes the waveform of the signal, leading to erroneous readings. The elimination of this noise is performed by different filtering techniques, where the adaptive filtering using the LMS (least mean squares) algorithm stands out. The objective of this article is to determine which algorithms best deal with motion artifacts, taking into account the use of instruments or wearable equipment, in different conditions of physical activity. A comparison between different algorithms derived from LMS (NLMS, PNLMS and IPNLM) used in adaptive filtering is carried out using indicators such as: Pearson's Correlation Coefficient, Signal to Noise Ratio (SNR) and Mean Squared Error (MSE) as metrics to evaluate them. For this purpose, the mHealth database was used, which contains ECG signals taken during moderate to medium intensity physical activities. The results show that filtering by IPNLMS as well as PNLMS offers an improvement both visually and in terms of SNR, Pearson, and MSE indicators.

1. INTRODUCTION

An ECG signal is generated by the cardiac muscle, it is also the electrical representation of the functioning of the heart and therefore has an important role in the diagnosis of heart disease, as well as in various physical performance tests in order to know the limit of cardiac functions of an individual. It is in these tests where the equipment or instruments to obtain the signals can be wearable and, being less lighter and less complex, it is optimal to reduce

---
* Universidad Nacional de San Agustín de Arequipa, School of Production and Services, Department of Electronic Engineering, Peru, jgaldosb@unsa.edu.pe, nlopezcol@unsa.edu.pe, amedinarodr@unsa.edu.pe, jhuarcaq@unsa.edu.pe, jrendulich@unsa.edu.pe, esullae@unsa.edu.pe

the computational cost of the equipment (Xu et al., 2019) since such instruments are located in places such as the wrist, chest or forehead (Medina et al., 2022). Therefore there will be a greater presence of motion artifacts. Signals obtained with an electrocardiograph are often contaminated by noise, which leads to an alteration in the expected waveform, making it difficult to read and interpret the signal. Some of the most common noises in ECG signals are: Baseline drift, Powerline Interference and Motion Artifact (Friesen et al., 1990).

Baseline Drift is very often caused by the breathing of the individual on whom the ECG signal is being taken. It is also represented as a sinusoidal component added to the ECG signal itself. Typically, it is found between the range of 0.15 and 0.30 Hz (Meyer & Keiser, 1977), (Sörnmo & Laguna, 2005). The Powerline interference is originated by the electrical network, represented by a sinusoidal signal at 60Hz and his respective harmonics (Levkov et al., 2005; Sörnmo & Laguna, 2005; Van Alsté & Schilder, 1985); and, Motion Artifact, which has a transient effect, originated by electrode displacement and physical movement of the individual. Typically, the amplitude of noise is less than 500\% of the peak-to-peak amplitude of the signal (Friesen et al., 1990).

Motion Artifact is considered the most difficult ECG noise to eliminate because the noise spectrum overlaps with the ECG signal taken (Thakor & Zhu, 1991). In addition, due to its dynamic nature, in many cases the noise is even greater in amplitude than the ECG signal. Motion Artifact is concentrated in the range of 0 to 5 Hz and is produced by the displacement of electrodes on the surface of the skin when performing physical movements such as walking or running (Xiong et al., 2019). Although Motion Artifact is typically associated with ECG signals, it can also manifest itself in PPG (Welhenge1 et al., 2019) signals or other physiological signals such as EMG (Boyer et al., 2023). This observation not only expands our understanding of the nature of this type of noise, but also contributes to a better understanding of its behavior, which is essential for research focused on denoising ECG signals.

The research to eliminate motion artifact from ECG signals has taken two main directions: eliminating noise from the source by designing new types of electrodes (Cömert & Hyttinen, 2015; Lee & Yun, 2017) or sensors (Kalra et al., 2024) that consider the conductivity of tissues and skin; and the removal of noise in the signal with a variety of techniques and filters. Techniques such as FIR (Finite Impulse Response) and IIR (Infinite impulse response) filter in its Butterworth high-pass version obtained an SNR improvement of 15 dB between the filtered signal and the clean signal (An & Stylios, 2020); (Jung & Jeong, 2013); the use of EMD (empirical mode decomposition) is shown in where a decomposition of the motion noise in the ECG signal is made for its subsequent elimination; wavelet-based denoising techniques, such as the one used in (Xiong et al., 2020) remove irrelevant information from the noise in order to obtain a better correlation with its reference signal and adaptive algorithms such as RLS (Recursive Least Squares) or LMS (Least Mean Squares) showed better performance compared to previously described techniques (An & Stylios, 2020), adaptive algorithms are usually accompanied by a reference signal, which is necessary and is obtained by various types of sensors such as inertial (Yoon et al., 2008), optical (Liu & Pecht, 2011) and pressure sensors (Xu et al., 2011). The choice of the type of sensor and the reference signal requiring an adaptive algorithm led to a comparison between the different types of sensors under the same conditions, where the signals obtained by an accelerometer and a gyroscope have a better performance in the different parameters measured, as well as a better correlation with the motion artifact affecting the ECG signals

(Lilienthal & Dargie, 2021). The use of an accelerometer signal as a reference signal for adaptive filtering is widely known from the use of single-axis accelerometers (Raya & Sison, 2002) to the 3-axis accelerometers used today; thus, the accelerometer signal is the most common reference signal. In addition to the mentioned strategies, some researchers have explored alternative approaches to address the problem of motion artifacts in ECG signals. The work developed by (Faiz & Kale, 2022) proposes the use of cascaded multistage adaptive noise cancellers of LMS algorithms and their variants. It is also possible to consider variations of the aforementioned strategies since it can also be considered as a Impedance Pneumography Signal (An et al., 2022) as a reference signal.

Nowadays, wearable biomedical devices such as electrocardiographs and PPG sensors are used in the sports field (Han et al., 2022). They offer extremely important parameters for the physical performance of athletes. These devices are also used in the medical field (Seok et al., 2021), where the so-called stress tests to patients to find or discard cardiovascular diseases play a very important role in the final diagnosis by the health professional (Medina et al., 2022). Both applications share a common factor: physical exercise as the main focus. The presence of movements generated by physical exercise, as explained above, generates motion artifact due to the displacement of electrodes, which is reflected in the signals obtained through biomedical devices, being the waveform of ECG signals in particular, contaminated with this type of noise (Seok et al., 2021). The Least Mean Squares algorithm together with its derivatives Normalized Least Mean Squares (NLMS), Proportionate Normalized Least Mean Squares (PNLMS) and Improved Proportionate Normalized Least Mean Squares (IPNLMS) are frequently used in motion noise reduction. In addition, numerous studies focusing on motion noise removal using LMS algorithms have been carried out (Kim et al., 2012; Xiong et al., 2019; Huang et al., 2019). However, the amount of works focused only on eliminating the motion artifact produced by sudden movement due to high-intensity physical exercise is limited.

The objective of this article is to determine which algorithms best deal with motion artifacts, taking into account the use of instruments or wearable equipment, in different conditions of physical activity. Thus, in the present work the authors propose the evaluation of LMS algorithms (NLMS, PNLMS and IPNLMS) in the elimination of motion artifact to determine which algorithm offers the best performance in a scenario of moderate and intense physical activity. The evaluation used ECG signals previously taken from the M-health database (Banos et al., 2014, 2015), which were divided into moderate and intense physical activity, and then the algorithms were applied one by one. The resulting signals were then compared with clean segments using non-subjective indicators (MSE, SNR, Pearson's Correlation Coefficient) to obtain values to determine which algorithm is better at removing motion artifact.

2. ADAPTIVE FILTERING

Signals contaminated with motion artifact are useless to clinicians or people in charge of making conclusions from these graphs, which is why the need to mitigate noise with the best method is of utmost importance. Adaptive algorithms are the ones that show the best performance for noise reduction (An & Stylios, 2020; Widrow et al., 1975), however, when it comes to choosing one, two main ones emerge: LMS and RLS (Ebrahimzadeh et al., 2015).
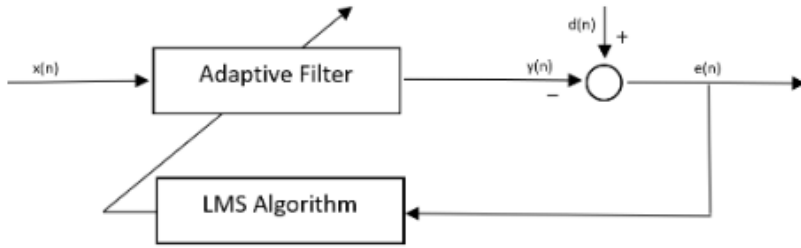
Fig. 1. Structure of LMS Algorithm based on the one showed in (Fang et al., 2019)

The LMS algorithm is an iterative algorithm focused on reducing the mean square error by updating the weights of its coefficients, widely used for its simplicity. The structure of the LMS algorithm is defined in Fig. 1, where the variables y(n), w(n) and the error e(n) are defined by (1), (2) and (3) respectively (Wittenmark, 2014):

$$y(n) = W^T(n)x(n) \tag{1}$$

$$e(n) = d(n) - y(n) \tag{2}$$

$$W(n + 1) = W(n) + \mu e(n)x(n) \tag{3}$$

The RLS algorithm is an algorithm where, given the least squares estimation of the vector of weights w(n), the updated estimation of this vector is calculated at n-iteration when new data is received. This algorithm outperforms the LMS algorithm in convergence speed but at a high computational cost, where the variables used are defined by (Tejaswi et al., 2020):

$$y(n) = W^T(n)x(n) \tag{4}$$

$$e(n) = d(n) - y \tag{5}$$

$$W(n) = W(n - 1) + \xi(n)[d(n) - W^T(n)x(n)] \tag{6}$$

Where ξ is the gain coefficient. While both algorithms help to eliminate motion noise, there are marked differences between the two as detailed in Table 1.

Tab. 1. Main differences between LMS and RLS

	Complexity	Convergence Speed
LMS	2N+1 Multiplications	Slow
RLS	4N+1 Multiplications	Fast

Thus, each one outstands in one of the two categories, however, since wearable devices are involved, the computational load is a very important factor, so the use of the algorithm with the lowest level of complexity, the LMS algorithm, will be preferred.

The LMS algorithm is used in many works aimed at eliminating motion noise in ECG signals. The use of this algorithm ranges from the simplest application to its use in cascaded stages (Kim et al., 2012) and combination with other methods (Xiong et al., 2019). In addition, in recent years, algorithms derived from the original LMS algorithm have been developed.

2.1. NLMS (Normalized Least Mean Squares)

The normalized LMS improves the stability and speed of convergence compared to the regular LMS algorithm (Slock, 1993). Thus, each coefficient of the applied filter is affected by a variable μ, typically between $0 < \mu < 2$, being a step size that directly affects the speed of convergence. The update of each coefficient is defined as follows:

$$W(n + 1) = W(n) + \frac{\mu x(n)e(n)}{x^T(n)x(n)} \tag{7}$$

2.2. PNLMS (Proportionate Normalized Least Mean Squares)

In this algorithm, the gain in each update is proportional to each tap position, resulting in a very fast convergence speed and assured stability (Duttweiler, 2000). For this purpose, a new step size "G" is added for gain as:

$$W(n + 1) = W(n) + \frac{\mu x(n)e(n)G(n + 1)}{x^T G(n + 1)x(n)} \tag{8}$$

$$G(n + 1) = diag[g_1(n + 1) + \cdots + g_L(n + 1)] \tag{9}$$

Where g_l is defined by:

$$\psi(n) = \frac{1}{L}\sum_{l=1}^{L} \psi_l(n) \tag{10}$$

$$\psi_l(n) = \max\{\rho \, max[\delta, ||W(n)||_\infty, |W_l(n)|]\} \tag{11}$$

$$g_l = \frac{\psi_i(n)}{\psi(n)} \tag{12}$$

For $l = 1, 2, 3.... L$ And the values of ρ and δ are added to avoid the first coefficient being zero

2.3. IPNLMS (Improved Proportionate Normalized Least Mean Squares)

This algorithm employs both PNLMS and NLMS update techniques, where an α control factor is added to the gain equation, typically between the ranges of $-1 < \alpha < 1$ (Benesty & Gay, 2002). The gain equation is now replaced by:

$$g_l(n+1) = \frac{1-\alpha}{2L} + (1+\alpha)\frac{|W_l(n)|}{2|\sum_0^l W_l(n)|} \qquad (13)$$

3. METODOLOGY

3.1. Database

For the testing stage, it was decided to use open source databases. They provide information on the protocol used, that is, under what conditions they were carried out, among which those required for the tests are that they contain ECG signals, which have been recorded during physical tests or (stress tests) use wearable sensors, and position sensors or accelerometers (as a reference signal). As an example there are databases such as Phisyonet (Goldberger et al., 2000) or IEE World CUP (Zhang et al., 2015). For the execution of the experiment, it is proposed to use the MHealth database (Banos et al., 2014, 2015). An open-source database used in several studies focused on the reduction of motion artifact in ECG signals, such as (Ghaleb et al., 2018b; Ghaleb et al., 2018a). This database collects the vital signs of ten volunteers of diverse profile during 12 physical activities, from walking to running and jumping, using Shimmer 3 (Burns et al., 2010) as a wearable device to collect the signals with a sampling rate of 50 Hz. Among the signals collected are ECG, accelerometer, magnetometer and gyroscope.

The signals needed for the experiment are the ECG signal and the accelerometer signal as a reference signal to be used as the reference signal in the adaptive filtering. From the ECG signals of each subject, two types of segments will be extracted, a segment with moderate motion artifact contamination when the subject walks and a segment with heavy motion artifact contamination, when the subject runs. A view of the waveform from two types of segments is shown in Fig. 2. Both signals will then go through adaptive filtering using derivatives of the LMS algorithm (NLMS, PNLMS and IPNLMS); the filtered result will be compared with a clean segment of the initial signal where the subject is resting using tools such as SNR, Pearson correlation coefficient and MSE as evaluation metrics.
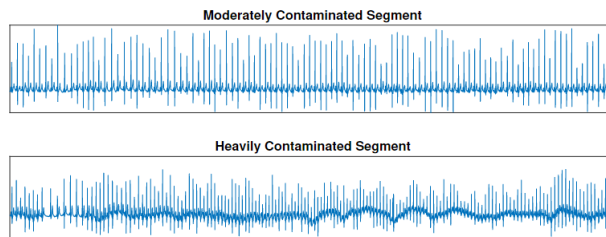

Fig. 2. Signals taken from the dataset segmented by moderately and heavily contamination

3.2. Indicators

The effectiveness of noise elimination filters and algorithms is subject to both objective and subjective evaluations, in this case. The use of different indicators in an objective manner allows to have a quantitative view of their performance. In addition, the following objective indicators have been used as tools to evaluate different filtering techniques applied to ECG signals (Mandala et al., 2017; Milanesi et al., 2008; Sultana et al., 2015; Yadav et al., 2021).

3.2.1. Signal to Noise Ratio variation (SNR)

The signal to noise ratio (SNR) variation shows the ratio of the signal to the noise that interferes with it, usually presented as a value in dB. A high value indicates that the signal is stronger than the existing noise. To evaluate the change in a signal that was contaminated with the signal that has been processed by the algorithm, the change in the SNR values obtained is considered. It is typically defined as:

$$\Delta SNR - 10 log\Delta \left(\frac{\sum x(n)^2}{\sum \left(\bar{x}(n) - x(n) \right)^2} \right) \\ - 10 log\Delta \left(\frac{\sum y(n)^2}{\sum \left(\bar{y}(n) - y(n) \right)^2} \right) \tag{14}$$

3.2.2. Mean Squared Error (MSE)

Mean Squared Error (MSE) provides the average of the difference of squares between the desired signal and the signal to be evaluated, in this case a value very close to 0 indicates a very good filtering job between two signals. MSE is defined as:

$$MSE = \frac{1}{N} \sum_{n-1}^{N} (x(n) - y(n))^2 \tag{15}$$

3.2.3. Pearson's correlation coefficient

The Pearson Correlation coefficient indicates the linear dependence of two signals In the case of ECG signals, a clean signal and a filtered signal in its entirety should have a coefficient of approximately 1. If the value obtained is zero or very close to zero, it is indicated that both signals do not have any type of correlation between them. The Pearson Correlation coefficient is defined as:

$$Pearson = \frac{\sigma xy}{\sigma x \sigma y} \tag{16}$$

To ensure better results, it is necessary to align the signals being compared, which is why DTW (Dynamic Time Warping) is used as an alignment tool, since it offers a non-linear alignment, as well as a good performance, especially in ECG signals (Huang & Kinsner, 2002; Tuzcu & Nas, 2005). The experimental procedure described above is carried out according to Fig. 3. Starting with segmenting the signals into moderately and heavily contaminated segments, the signals are then run through the derived LMS algorithms, and the resulting signal is then compared to a clean signal segment using non-subjective metrics to obtain the final data.
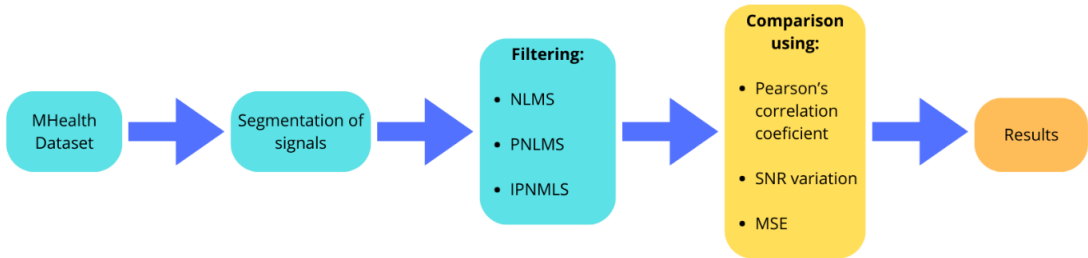

Fig. 3. Block Diagram of the Procedure

4. RESULTS

The results obtained by SNR for the 10 subjects are shown in Tables 2 and 3. The results for MSE are shown in Tables 4 and 5. In the case of Pearson's correlation coefficient, the results son multiplied by 100 for an analysis in percentages, the results are shown in Tables 6 and 7.The comparison will be performed by taking an average of the 10 results for the 10 signals evaluated in each category: moderate and heavily contaminated, as well as in each indicator, and the corresponding LMS derivative.

The Tables compare the results of the 10 test subjects with the 3 algorithms used for filtering according to the non-subjective indicators mentioned. In Tables 2 and 3, the SNR indicator is used, according to the values found, the lighter the color, the greater noise elimination has been achieved in the signal. Observing Table 2, the signals that have moderate contamination have been used due to the moderate intensity of the physical test, with the NLMS algorithm being mostly the best results. Finally, in Figure 4, the SNR values are seen in a bar graph and the improvement of the algorithms compared to the values of the original signal is visually observed. There are better results with the NLMS algorithm in general.

Tab. 2. SNR Variation for moderately contaminated signals in db

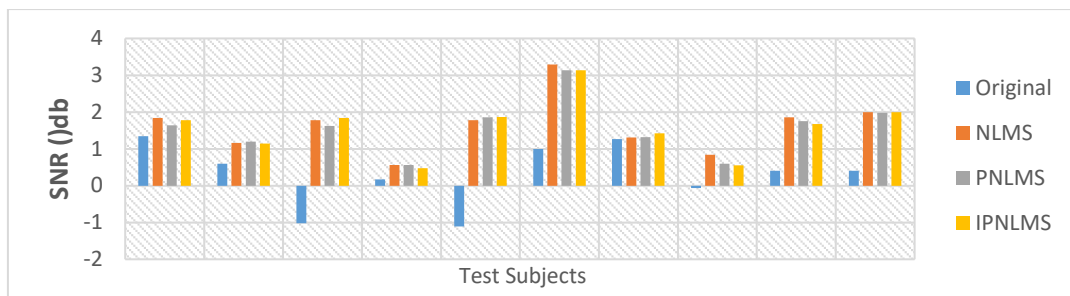|	Subject 1	Subject 2	Subject 3	Subject 4	Subject 5	Subject 6	Subject 7	Subject 8	Subject 9	Subject 10
Original	1.343	0.593	-1.018	0.173	-1.104	1	1.267	-0.068	0.407	0.407
NLMS	1.841	1.164	1.776	0.564	1.775	3.289	1.313	0.84	1.857	2
PNLMS	1.642	1.198	1.624	0.563	1.858	3.134	1.317	0.592	1.754	1.976
IPNLMS	1.783	1.143	1.84	0.474	1.867	3.138	1.426	0.55	1.678	1.992

Fig. 4. SNR comparison graph of the original signal and the result of the 3 algorithms in Table 2 (they are ordered from subject 1 to 10 from left to right)

On the other hand, as shown in Table 3, the original signal presents greater contamination in the signal, taking on more intense colors, due to the high intensity of the physical test. Consequently, negative SNR values are seen, which after being treated by the algorithms yield positive results; likewise, the algorithm with the best results would be the NLMS algorithm. Furthermore, Figure 5 visually shows the result being satisfactory, although there are greater cases of negative SNR.

Tab. 3. SNR improvement for heavily contaminated signals in db

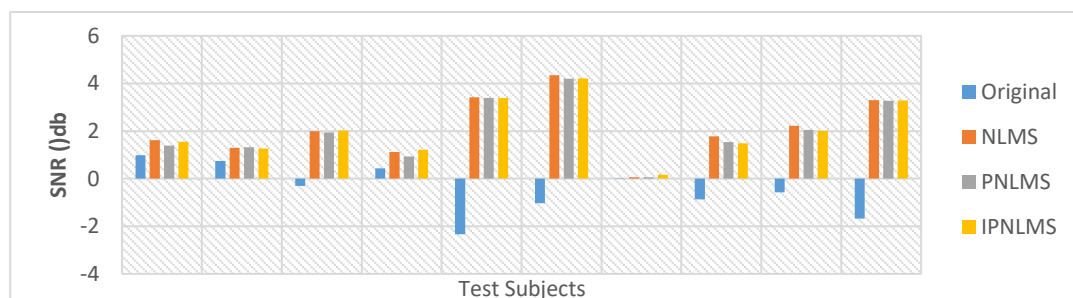|	Subject 1	Subject 2	Subject 3	Subject 4	Subject 5	Subject 6	Subject 7	Subject 8	Subject 9	Subject 10
Original	0.989	0.745	-0.304	0.437	-2.34	-1.031	-0.002	-0.866	-0.575	-1.673
NLMS	1.615	1.294	1.991	1.123	3.424	4.344	0.057	1.777	2.218	3.301
PNLMS	1.39	1.323	1.939	0.93	3.394	4.194	0.061	1.538	2.044	3.267
IPNLMS	1.556	1.268	2.018	1.219	3.391	4.208	0.172	1.487	2.003	3.28

Fig. 5. SNR comparison graph of the original signal and the result of the 3 algorithms in Table 3 (they are ordered from subject 1 to 10 from left to right)

In addition, Tables 4 and 5 show the data from the calculation of the MSE indicator in the original signal and in the signal after being processed using the algorithms. Keeping in mind that the closer the value of the MSE indicator is to 0, the better the use of the algorithms will have been. Therefore, the closer the value is to 0, the lighter the color of the cell will be and the higher the value, the more intense the green color will be. Table 4 indicates the moderate intensity of the test, with test subjects 1 to 5 and 7 having positive results.

Tab. 4. MSE for moderately contaminated signals

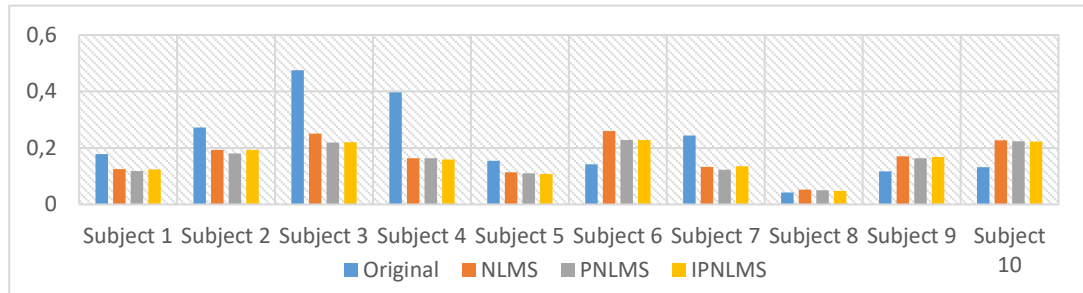|	Subject 1	Subject 2	Subject 3	Subject 4	Subject 5	Subject 6	Subject 7	Subject 8	Subject 9	Subject 10
Original	0.1788	0.2722	0.4747	0.397	0.1547	0.1425	0.2436	0.0421	0.1177	0.132
NLMS	0.1256	0.1927	0.251	0.1637	0.1132	0.2597	0.1325	0.0527	0.1708	0.2268
PNLMS	0.1185	0.181	0.2187	0.164	0.1104	0.2281	0.1233	0.0505	0.1641	0.2236
IPNLMS	0.1236	0.1931	0.2202	0.1588	0.1084	0.228	0.1348	0.0485	0.168	0.2224

Fig. 6. MSE comparison graph of the original signal and the result of the 3 algorithms in Table 4

In contrast, Table 5 compares the MSE indicator data of the original signal and the signals processed by the algorithms during more intense physical tests generating more noise. It should be added that, except for patient 7, all have managed to reduce the MSE of the contaminated signal.

Tab. 5. MSE for heavily contaminated signals

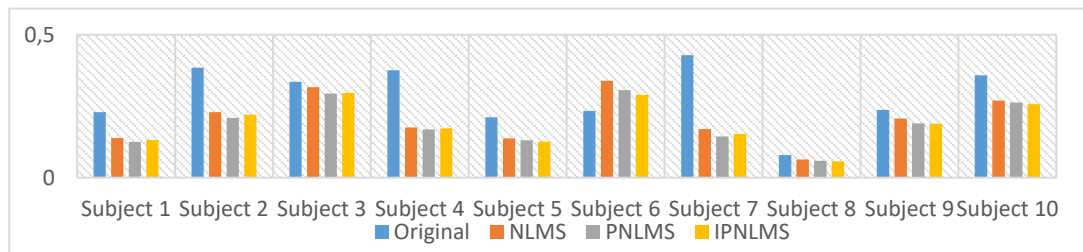|	Subject 1	Subject 2	Subject 3	Subject 4	Subject 5	Subject 6	Subject 7	Subject 8	Subject 9	Subject 10
Original	0.2296	0.3844	0.3361	0.3765	0.211	0.2336	0.4286	0.0791	0.2373	0.3585
NLMS	0.1382	0.229	0.3164	0.1759	0.1378	0.3385	0.1704	0.0637	0.2071	0.2697
PNLMS	0.125	0.2086	0.2938	0.1691	0.1313	0.307	0.1446	0.0594	0.1897	0.2625
IPNLMS	0.1316	0.2204	0.2966	0.1725	0.1261	0.2902	0.1528	0.057	0.1894	0.2573

Fig. 7. MSE comparison graph of the original signal and the result of the 3 algorithms in Table 4

Finally, the Pierson coefficient is presented as a percentage in Tables 6 and 7. Therefore, in order to determine whether positive results were obtained, the blue colors will be more intense, the lower the percentage of calculations was obtained, that is, the higher the percentage, the greater the effectiveness of the filters used. In Figure 7, it can be seen that

the filters were effective, as the percentage value increased significantly compared to the original signal of each test subject.

Tab. 6. Pearson's correlation coefficient for moderately contaminated signals (%)

|	Subject 1	Subject 2	Subject 3	Subject 4	Subject 5	Subject 6	Subject 7	Subject 8	Subject 9	Subject 10
Original	80.0408	81.0646	85.0055	78.0672	89.8877	81.0026	84.7581	91.0449	85.8875	85.6068
NLMS	87.9365	86.5391	90.8545	90.8264	91.6918	78.3434	92.1593	90.0947	84.6834	81.7255
PNLMS	88.1843	87.2972	91.3917	90.5569	91.9526	80.0354	92.6596	89.8264	84.7703	81.8304
IPNLMS	87.9241	86.4691	91.4443	90.6238	91.9122	80.0461	92.0405	90.0359	84.0459	81.9593
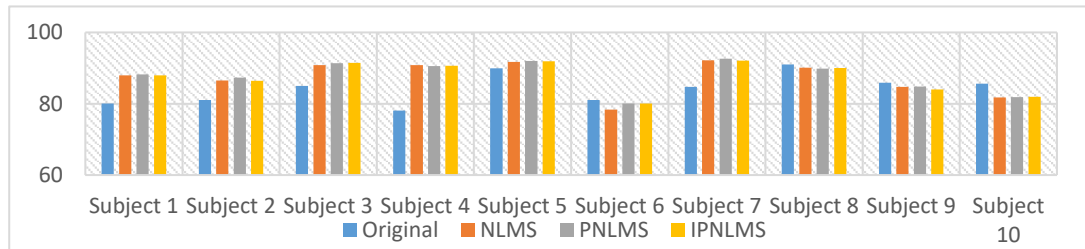
Fig. 8. MSE comparison graph of the original signal and the result of the 3 algorithms in Table 6

On the other hand, in Table 7 the Pierson coefficient of the original signal on average is slightly lower than the Pierson coefficient of Table 6 (84.23% vs 81.04%) because in Table 7 the physical test of greater intensity, and it is shown that in Figure 8, the difference in the percentage of the coefficient between the original signal and the signals treated with the algorithms is not so marked, yet positive results were obtained.

Tab. 7. Pearson's correlation coefficient for heavily contaminated signals (%)

|	Subject 1	Subject 2	Subject 3	Subject 4	Subject 5	Subject 6	Subject 7	Subject 8	Subject 9	Subject 10
Original	81.4683	78.9213	80.9762	76.0117	89.6946	74.7383	82.1124	86.6918	80.5793	79.2391
NLMS	88.9683	85.3149	83.2761	88.7742	88.8228	73.8097	91.8993	88.3789	83.9937	81.3969
PNLMS	89.2573	86.137	83.5408	88.522	89.0533	74.718	92.5531	88.2812	83.9573	81.4883
IPNLMS	88.9327	85.3073	83.3916	88.7122	89.3907	75.5052	91.9474	88.5503	83.5403	81.7063
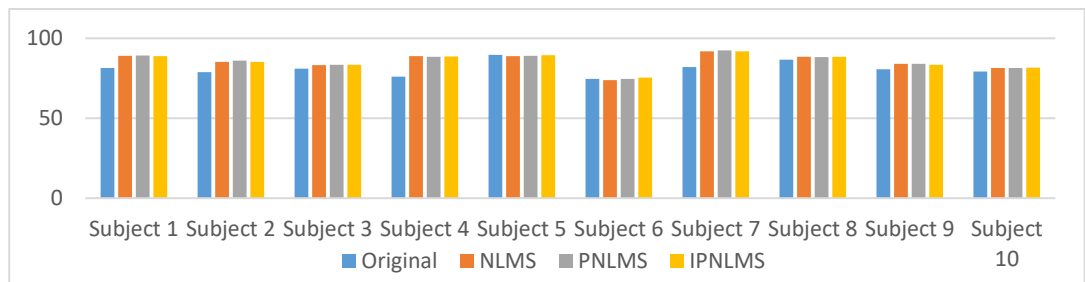
Fig. 9. MSE comparison graph of the original signal and the result of the 3 algorithms in Table 7

5. DISCUSSION

Tables 2 and 3 show the variation in SNR for moderately and heavily contaminated signals, where the largest and therefore most noticeable positive change is reflected in the tests performed on heavily contaminated signals. The results shown in Tables 4 and 5 show the MSE values obtained for signals contaminated by motion artifact moderately and heavily respectively; from the values obtained, smaller MSE values are observed as the signals pass through the LMS algorithms in the 80% percentile of the signals considered. Tables 6 and 7 show the results obtained after obtaining the Pearson's correlation coefficient for moderately and heavily contaminated signals with motion artifact. The results obtained show a greater improvement in the correlation of the heavily contaminated signals with the clean reference signal in comparison with results of the moderately contaminated signals.

Tab. 8. Comparative table of the results of the indicators (SNR, MSE, and Pierson's coefficient)

	SNR		MSE		Pearson's coefficient	
	Moderately Contaminated	Heavily Contaminated	Moderately Contaminated	Heavily Contaminated	Moderately Contaminated	Heavily Contaminated
Original	0.3001	-0.4621	0.2155	0.2874	84.2366	81.0433
NLMS	1.642	2.1145	0.1689	0.2047	87.4855	85.4635
PNLMS	1.5657	2.0081	0.1582	0.1891	87.8505	85.7508
IPNLMS	1.5891	2.0601	0.1606	0.1894	87.6501	85.6984

Finally, Table 8 shows averaged values for each category using the results of Tables 2 to 7 with moderately and heavily contaminated signals. The results obtained using SNR, MSE and Pearson's correlation coefficient show that on average, PNMLS and IPNLMS perform better in suppressing motion artifact compared to the results obtained by NMLS. In addition, the IPNLMS algorithm offers subtle improvements in SNR results when compared to PNLMS for moderately and heavily contaminated signals with values of 1.589 and 2.0601 db vs. 1.566 and 2.008 db. However, PNLMS is better than IPNLMS in MSE (0.158 and 0.1891 vs. 0.160 and 0.1894) and Pearson Correlation Coefficient (87.850 and 85.750 vs. 87.650 and 85.698), thus, PNLMS is the best performing algorithm considering that IPNLMS generates more computational load with a very small benefit compared to PNLMS. In general, there is a noticeable improvement in visual terms when doing the NLMS, PNLMS and IPNLMS filtering as shown in Fig 9. Figure 9A shows the original signal with heavy motion artifact, Figure 9B is the contaminated signal after passing through the NLMS algorithm. Figure 9C is the contaminated signal after passing through the PNLMS algorithm and Figure 9D is the signal after passing through the IPNLM algorithm. The most evident visual improvement is seen in the graph of the signal after PNLMS and IPNLMS filtering.
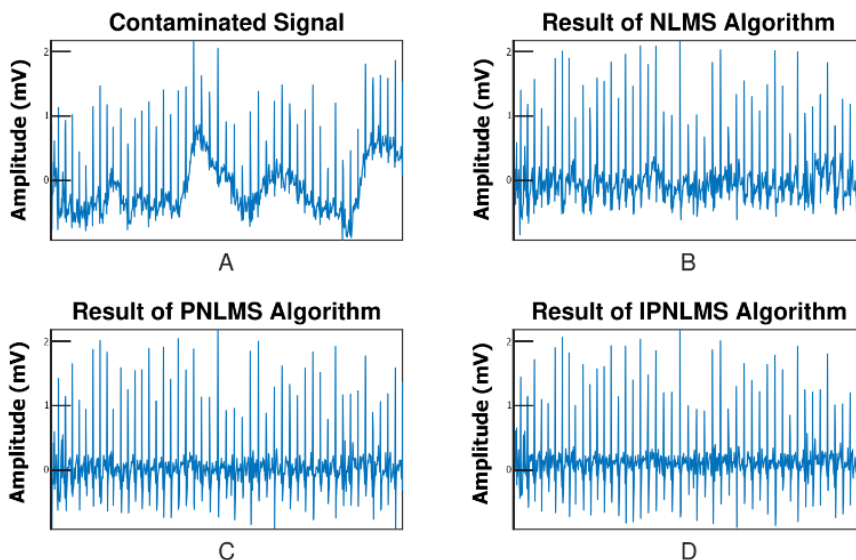
Fig. 10. Visual improvement in each algorithm. (A) Contaminated Signal, (B) Signal after NLMS algorithm, (C) Signal after PNLMS algorithm, (D) Signal after IPNLMS algorithm

6. CONCLUSION

A comparison of LMS-based filtering algorithms applied to ECG signals contaminated with motion artifacts resulting from different exercise intensities yielded significant results that may have implications for improving cardiovascular disease diagnosis processes, especially those using cardiac exercise testing. The research revealed that while all algorithms demonstrated some efficacy in mitigating motion artifact, the PNLMS algorithm emerged as the most effective in filtering out noise induced by exercise, as evidenced by superior results in visual analysis (Figure 9) and objective indicators like MSE, SNR, and the Pearson Correlation Coefficient. This highlights the potential of PNLMS-based approaches to enhance the quality of ECG data acquired during physical activity, thereby improving the precision of cardiovascular evaluations that use sensors or wearable instruments and in addition to reference signals (accelerometer, gyroscope or inertial sensors).

In the future, it would be beneficial to create a specialized database specifically targeting movement artifacts induced by various exercise intensities or cardiac stress testing protocols. This database could facilitate more precise evaluations of filtering algorithms. Additionally, exploring the use of different contact points for sensors or electrodes during data acquisition could offer valuable insights into optimizing signal quality.

Moreover, upcoming research endeavors should delve into integrating advanced filtering techniques, such as machine learning, with the adaptive algorithms discussed. This integration holds the potential to significantly enhance the efficacy of motion artifact removal, paving the way for more accurate and reliable physiological signal analysis.

REFERENCES

An, X., Liu, Y., Zhao, Y., Lu, S., Stylios, G. K., & Liu, Q. (2022). Adaptive motion artifact reduction in wearable ECG measurements using impedance pneumography signal. *Sensors*, *22*(15). https://doi.org/10.3390/s22155493

An, X., & Stylios, G. K. (2020). Comparison of motion artefact reduction methods and the implementation of adaptive motion artefact reduction in wearable electrocardiogram monitoring. *Sensors*, *20*(5). https://doi.org/10.3390/s20051468

Banos, O., Garcia, R., Holgado-Terriza, J. A., Damas, M., Pomares, H., Rojas, I., Saez, A., & Villalonga, C. (2014). mHealthDroid: A novel framework for agile development of mobile health applications. In L. Pecchia, L. L. Chen, C. Nugent, & J. Bravo (Eds.), *Ambient Assisted Living and Daily Activities* (pp. 91–98). Springer International Publishing. https://doi.org/10.1007/978-3-319-13105-4_14

Banos, O., Villalonga, C., Garcia, R., Saez, A., Damas, M., Holgado-Terriza, J. A., Lee, S., Pomares, H., & Rojas, I. (2015). Design, implementation and validation of a novel open framework for agile development of mobile health applications. *BioMedical Engineering OnLine*, *14*(2), S6. https://doi.org/10.1186/1475-925X-14-S2-S6

Benesty, J., & Gay, S. L. (2002). An improved PNLMS algorithm. *2002 IEEE International Conference on Acoustics, Speech, and Signal Processing* (pp. 1881–1884). IEEE. https://doi.org/10.1109/icassp.2002.5744994

Boyer, M., Bouyer, L., Roy, J. S., & Campeau-Lecours, A. (2023). Reducing noise, artifacts and interference in single-channel EMG signals: A review. *Sensors*, *23*(6), 2927. https://doi.org/10.3390/s23062927

Burns, A., Greene, B. R., McGrath, M. J., O'Shea, T. J., Kuris, B., Ayer, S. M., Stroiescu, F., & Cionca, V. (2010). SHIMMER^{TM} - A wireless sensor platform for noninvasive biomedical research. *IEEE Sensors Journal*, *10*(9), 1527–1534. https://doi.org/10.1109/JSEN.2010.2045498

Cömert, A., & Hyttinen, J. (2015). A motion artifact generation and assessment system for the rapid testing of surface biopotential electrodes. *Physiological Measurement*, *36*, 1. https://doi.org/10.1088/0967-3334/36/1/1

Duttweiler, D. L. (2000). Proportionate normalized least-mean-squares adaptation in echo cancelers. *IEEE Transactions on Speech and Audio Processing*, *8*(5), 508–518. https://doi.org/10.1109/89.861368

Ebrahimzadeh, E., Pooyan, M., Jahani, S., Bijar, A., & Setaredan, S. K. (2015). ECG signals noise removal: Selection and optimization of the best adaptive filtering algorithm based on various algorithms comparison. *Biomedical Engineering - Applications, Basis and Communications*, *27*(4), 1550038. https://doi.org/10.4015/S1016237215500386

Faiz, M. M. U., & Kale, I. (2022). Removal of multiple artifacts from ECG signal using cascaded multistage adaptive noise cancellers. *Array*, *14*, 100133. https://doi.org/10.1016/j.array.2022.100133

Fang, Y., Zhu, X., Gao, Z., Hu, J., & Wu, J. (2019). New feedforward filtered-x least mean square algorithm with variable step size for active vibration control. *Journal of Low Frequency Noise Vibration and Active Control*, *38*(1), 187–198. https://doi.org/10.1177/1461348418812326

Friesen, G. M., Jannett, T. C., Jadallah, M. A., Yates, S. L., Quint, S. R., & Nagle, H. T. (1990). A comparison of the noise sensitivity. *IEEE. Transactions on Biomedical Engineering*, *37*(1), 85-98. https://doi.org/10.1109/10.43620

Ghaleb, F. A., Kamat, M. B., Salleh, M., Rohani, M. F., & Razak, S. A. (2018a). Two-stage motion artefact reduction algorithm for electrocardiogram using weighted adaptive noise cancelling and recursive Hampel filter. *PLoS ONE*, *13*(11), e0207176. https://doi.org/10.1371/journal.pone.0207176

Ghaleb, F. A., Kamat, M., Salleh, M., Rohani, M. F., & Hadji, S. E. (2018b). Motion artifact reduction algorithm using sequential adaptive noise filters and estimation methods for mobile ECG. In F. Saeed, N. Gazem, S. Patnaik, A. S. Saed Balaid, & F. Mohammed (Eds.), *Recent Trends in Information and Communication Technology* (pp. 116–123). Springer International Publishing. https://doi.org/10.1007/978-3-319-59427-9_13

Goldberger, A. L., Amaral, L. A., Glass, L., Hausdorff, J. M., Ivanov, P. C., Mark, R. G., Mietus, J. E., Moody, G. B., Peng, C. K., & Stanley, H. E. (2000). PhysioBank, PhysioToolkit, and PhysioNet: Components of a new research resource for complex physiologic signals. *Circulation*, *101*, e215–e220. https://doi.org/10.1161/01.cir.101.23.e215

Han, D., Bashar, S. K., Lázaro, J., Mohagheghian, F., Peitzsch, A., Nishita, N., Ding, E., Dickson, E. L., Dimezza, D., Scott, J., Whitcomb, C., Fitzgibbons, T. P., McManus, D. D., & Chon, K. H. (2022). A real-time PPG peak detection method for accurate determination of heart rate during sinus rhythm and cardiac arrhythmia. *Biosensors*, *12*(2), 82. https://doi.org/10.3390/bios12020082

Huang, B., & Kinsner, W. (2002). ECG frame classification using dynamic time warping. *Canadian Conference on Electrical and Computer Engineering (IEEE CCECE2002)* (pp. 105–1110). IEEE. https://doi.org/10.1109/ccece.2002.1013101

Huang, M., Chen, D., & Xiong, F. (2019). An effective adaptive filter to reduce motion artifacts from ECG signals using accelerometer. *9th International Conference on Biomedical Engineering and Technology (ICBET '19)* (pp. 83–88). Association for Computing Machinery. https://doi.org/10.1145/3326172.3326214

Jung, H. K., & Jeong, D. U. (2013). Development of wearable ECG measurement system using EMD for motion artifact removal. *7th International Conference on Computing and Convergence Technology (ICCCT)* (pp. 299-304). IEEE.

Kim, H., Kim, S., Van Helleputte, N., Berset, T., Geng, D., Romero, I., Penders, J., Van Hoof, C., & Yazicioglu, R. F. (2012). Motion artifact removal using cascade adaptive filtering for ambulatory ECG monitoring system. *2012 IEEE Biomedical Circuits and Systems Conference (BioCAS)* (pp. 160–163). IEEE. https://doi.org/10.1109/BioCAS.2012.6418472

Lee, J. W., & Yun, K. S. (2017). ECG monitoring garment using conductive carbon paste for reduced motion artifacts. *Polymers*, *9*(9), 439. https://doi.org/10.3390/polym9090439

Levkov, C., Mihov, G., Ivanov, R., Daskalov, I., Christov, I., & Dotsinsky, I. (2005). Removal of power-line interference from the ECG: A review of the subtraction procedure. *BioMedical Engineering Online*, *4*, 50. https://doi.org/10.1186/1475-925X-4-50

Lilienthal, J., & Dargie, W. (2021). Comparison of reference sensor types and position for motion artifact removal in ECG. *European Signal Processing Conference (EUSIPCO)* (pp. 1296–1300). IEEE. https://doi.org/10.23919/EUSIPCO54536.2021.9616221

Liu, Y., & Pecht, M. G. (2011). Reduction of motion artifacts in electrocardiogram monitoring using an optical sensor. *Biomedical Instrumentation and Technology*, *45*(2), 155–163. https://doi.org/10.2345/0899-8205-45.2.155

Mandala, S., Fuadah, Y. N., Arzaki, M., & Pambudi, F. E. (2017). Performance analysis of wavelet-based denoising techniques for ECG signal. *5th International Conference on Information and Communication Technology (ICoIC7)* (pp. 1-6). IEEE. https://doi.org/10.1109/ICoICT.2017.8074701

Kalra, A. M., Anand, G., Lowe, A., Simpkin, R., & Budgett, D. (2024). A smart idea to reject motion artefacts from ECG measurements due to sensor-body impedance. *Sensors and Actuators: A. Physical*, *367*, 114989. https://doi.org/10.1016/j.sna.2023.114989

Medina, A., Lopez, N., Galdos, J., Supo, E., Rendulich, J., & Sulla, E. (2022). Continuous blood pressure estimation in wearable devices using photoplethysmography: A Review. *International Journal of Emerging Technology and Advanced Engineering*, *12*(10), 104–113. https://doi.org/10.46338/ijetae1022_12

Meyer, C. R., & Keiser, H. N. (1977). Electrocardiogram baseline noise estimation and removal using cubic splines and state-space computation techniques. *Computers and Biomedical Research*, *10*(5), 459–470. https://doi.org/10.1016/0010-4809(77)90021-0

Milanesi, M., Martini, N., Vanello, N., Positano, V., Santarelli, M. F., & Landini, L. (2008). Independent component analysis applied to the removal of motion artifacts from electrocardiographic signals. *Medical and Biological Engineering and Computing*, *46*, 251–261. https://doi.org/10.1007/s11517-007-0293-8

Raya, M. A. D., & Sison, L. G. (2002). Adaptive noise cancelling of motion artifact in stress ECG signals using accelerometer. *Second Joint 24th Annual Conference and the Annual Fall Meeting of the Biomedical Engineering Society] [Engineering in Medicine and Biology]* (pp. 1756–1757). IEEE. https://doi.org/10.1109/iembs.2002.1106637

Seok, D., Lee, S., Kim, M., Cho, J., & Kim, C. (2021). Motion artifact removal techniques for wearable EEG and PPG sensor systems. *Frontiers in Electronics*, *2*, 685513. https://doi.org/10.3389/felec.2021.685513

Slock, D. T. M. (1993). On the convergence behavior of the LMS and the normalized LMS algorithms. *IEEE Transactions on Signal Processing*, *41*(9), 2811–2825. https://doi.org/10.1109/78.236504

Sörnmo, L., & Laguna, P. (2005). *Bioelectrical Signal Processing in Cardiac and Neurological Applications*. Elsevier Inc.

Sultana, N., Kamatham, Y., & Kinnara, B. (2015). Performance analysis of adaptive filtering algorithms for denoising of ECG signals. *2015 International Conference on Advances in Computing, Communications and Informatics (ICACCI)* (pp. 297–302). IEEE. https://doi.org/10.1109/ICACCI.2015.7275624

Welhenge1, A., Taparugssanagorn, A., & Raez, C. P. (2019). Performance comparison of variants of LMS algorithms for motion artifact removal in PPG signals during physical activities. *Biomedical Journal of Scientific & Technical Research*, *14*(1). https://doi.org/10.26717/bjstr.2019.14.002485

Tejaswi, V., Surendar, A., & Srikanta, N. (2020). Simulink implementation of RLS algorithm for resilient artefacts removal in ECG signal. *International Journal of Advanced Intelligence Paradigms*, *16*(3/4), 324–337. https://doi.org/10.1504/IJAIP.2020.107529

Thakor, N. V., & Zhu, Y. S. (1991). Applications of adaptive Filtering to ECG analysis: Noise cancellation and arrhythmia detection. *IEEE Transactions on Biomedical Engineering*, *38*(8), 785–794. https://doi.org/10.1109/10.83591

Tuzcu, V., & Nas, S. (2005). Dynamic time warping as a novel tool in pattern recognition of ECG changes in heart rhythm disturbances. *IEEE International Conference on Systems, Man and Cybernetics* (pp. 182–186). IEEE. https://doi.org/10.1109/icsmc.2005.1571142

Van Alsté, J. A., & Schilder, T. S. (1985). Removal of base-line wander and power-line interference from the ECG by an efficient FIR filter with a reduced number of taps. *IEEE Transactions on Biomedical Engineering*, *BME-32*(12), 1052–1060. https://doi.org/10.1109/TBME.1985.325514

Widrow, B., Williams, C. S., Glover, J. R., McCool, J. M., Hearn, R. H., Zeidler, J. R., Kaunitz, J., Dong, E., & Goodlin, R. C. (1975). Adaptive noise cancelling: Principles and applications. *IEEE*, *63*(12), 1692–1716. https://doi.org/10.1109/PROC.1975.10036

Wittenmark, B. (2014). Adaptive filter theory. Simon Haykin. *Automatica*, *29*(2), 567-568. https://doi.org/10.1016/0005-1098(93)90162-M

Xiong, F., Chen, D., Chen, Z., & Dai, S. (2019). Cancellation of motion artifacts in ambulatory ECG signals using TD-LMS adaptive filtering techniques. *Journal of Visual Communication and Image Representation*, *58*, 606–618. https://doi.org/10.1016/j.jvcir.2018.12.030

Xiong, F., Chen, D., & Huang, M. (2020). A wavelet adaptive cancellation algorithm based on multi-inertial sensors for the reduction of motion artifacts in ambulatory ECGs. *Sensors*, *20*(4), 970. https://doi.org/10.3390/s20040970

Xu, L., Rabotti, C., Zhang, Y., Ouzounov, S., Harpe, P. J. A., & Mischi, M. (2019). Motion-artifact reduction in capacitive heart-rate measurements by adaptive filtering. *IEEE Transactions on Instrumentation and Measurement*, *68*(10), 4085–4093. https://doi.org/10.1109/TIM.2018.2884041

Xu, P., Tao, X., & Wang, S. (2011). Measurement of wearable electrode and skin mechanical interaction using displacement and pressure sensors. *4th International Conference on Biomedical Engineering and Informatics (BMEI)* (pp. 1131–1134). IEEE. https://doi.org/10.1109/BMEI.2011.6098433

Yadav, S., Saha, S. K., Kar, R., & Mandal, D. (2021). Optimized adaptive noise canceller for denoising cardiovascular signal using SOS algorithm. *Biomedical Signal Processing and Control*, *69*, 102830. https://doi.org/10.1016/j.bspc.2021.102830

Yoon, S. W., Min, S. D., Yun, Y. H., Lee, S., & Lee, M. (2008). Adaptive motion artifacts reduction using 3-axis accelerometer in E-textile ECG measurement system. *Journal of Medical Systems*, *32*, 101–106. https://doi.org/10.1007/s10916-007-9112-x

Zhang, Z., Pi, Z., & Liu, B. (2015). TROIKA: A general framework for heart rate monitoring using wrist-type photoplethysmographic signals during intensive physical exercise. *IEEE Transactions on Biomedical Engineering*, *62*(2), 522–531. https://doi.org/10.1109/TBME.2014.2359372